Inverse Methods

Johannes Weickenmeier and Edoardo Mazza

Abstract The mechanical properties of skin have been studied for several decades; yet, to this day reported stiffness values for full-thickness skin or individual layers such as the epidermis, papillary dermis, reticular dermis, and subcutis vary drastically. In vivo and ex vivo measurement techniques include extension, indentation, and suction tests. At the same time, several new imaging modalities emerged that visualize tissue microstructure at length scales ranging from the cell to the organ level. Informed by the experimental characterization of mechanobiological skin properties, computational skin models aim at predicting the soft tissue response under various physiological conditions such as skin growth, scar tissue formation, and surgical interventions. The identification of corresponding model parameters plays a major role in improving the predictive capabilities of such constitutive models. Here, we first provide an overview of the most common measurement techniques and imaging modalities. We then discuss popular methods used for model parameter identification based on inverse methods.

1   Introduction

Skin mechanics has been studied for several decades [1]. The medical field is interested in diagnosis, monitoring, and treating skin diseases [2], preventing excessive scar tissue formation [3], and facilitating fast wound healing in wound care [4, 5]. Biomechanics aims at characterizing mechanical properties to model

J. Weickenmeier (✉)
Department of Mechanical Engineering, Stevens Institute of Technology, Hoboken, NJ, USA
e-mail: johannes.weickenmeier@stevens.edu

E. Mazza
Department of Mechanical and Process Engineering, ETH, Zurich, Switzerland

Swiss Federal Laboratories for Materials Science and Technology, EMPA, Duebendorf, Switzerland

skin deformation behavior, to provide criteria for developing artificial skin, or to simulate skin behavior in facial animations [6], skin wrinkling [7], analysis of congenital skin defects [8, 9], and personalized reconstructive surgery [10].

The multilayered anatomy of skin can be represented in corresponding biomechanical models and this leads to the requirement of determining layer specific constitutive equations [11]. Previous research provided a wide range of constitutive model formulations for skin, but to this day no generally accepted theory exists that translates microstructural tissue properties into corresponding model equations [12].

The comparability of models proposed in the literature is often limited due to significant differences in the representation of skin anatomy. Large discrepancies in predicted mechanical response are also linked with differences in the deformation modes considered for model development. In fact, model parameters are often determined based on data obtained from one specific experimental configuration. The range of validity of such parameter sets is inherently limited, in that an optimization may well reproduce the experiments for a particular loading condition but is likely to provide poor predictions for any generalized multiaxial, time dependent deformation state [13]. Skin literature presents several dedicated parameter identification schemes that combine a particular mechanical testing method with a skin model formulation representative of that experiment.

This review presents different procedures for skin characterization and associated model parameter identification schemes and discusses their limitations with regard to the development of a skin model of more general validity. The chapter briefly summarizes skin anatomy and outlines experimental methods suitable for a quantitative analysis of skin constituents at different length scales. We then describe common testing protocols for characterizing skin mechanical properties and outline corresponding structural and phenomenological models used for their analysis. Finally, we discuss inverse analysis procedures presented in skin literature addressing problems associated with the variability in experimental data, the contribution of individual skin layers, and the inherent coupling between model parameters.

2   Experimental Anatomy of Skin

The anatomy of skin has been studied extensively, and histochemical staining and dissection have led to a comprehensive description of cells and microstructure of individual skin layers; yet, to date the characterization of skin microstructure across spatial and temporal scales in its natural in vivo environment remains an active field of research. Many visualization techniques have been developed to study skin and its individual layers for a rich set of medically relevant applications and experimental investigations. Ultrasound and magnetic resonance imaging of skin at the organ level are common diagnostic tools in clinical practice and microscopy-based visualization methods are often used in research to study skin at the tissue and cellular level [14].

In view of skin modeling and the identification of corresponding parameters, it is relevant to differentiate between an anatomical description of skin and the actually experimentally observable microstructure with its associated properties [15]. Each imaging modality is generally limited to a specific length scale and it remains a major challenge to visualize skin anatomy in vivo from the organ level down to the cellular level [16].

In the following, we present a brief description of skin anatomy and summarize imaging modalities that visualize skin at the organ, tissue, and cellular level.

2.1 Anatomical Description

Figure 1 shows a representation of skin that consists of three main layers [18]: the outermost epidermis is typically 100 µm thick. The layer underneath, the dermis, is around 500 µm thick and consists of two sublayers: the papillary dermis and the reticular dermis. The deepest layer is the hypodermis with a thickness of around 1 mm. The actual size and microstructure of these individual layers varies with location in the body in order to provide optimal functionality, such as resilience in feet, grip in palms, and barrier function around the core body.

The epidermis protects the body against mechanical and microbacterial hazards and prevents the body from dehydration. The outermost layer, the stratum corneum, consisting of 5–10 layers of dead, keratin rich, and flat cells, represents a barrier impermeable to most biochemical and toxic compounds. The four additional layers underneath, often referred to as the viable or living epidermis, consist of cells that migrate from the dermal-epidermal junction and gradually die, whilst accumulating keratin and losing their nuclei. The dense cell layering gives the epidermis significant mechanical strength and often plays an important role in the response observed in skin tests.
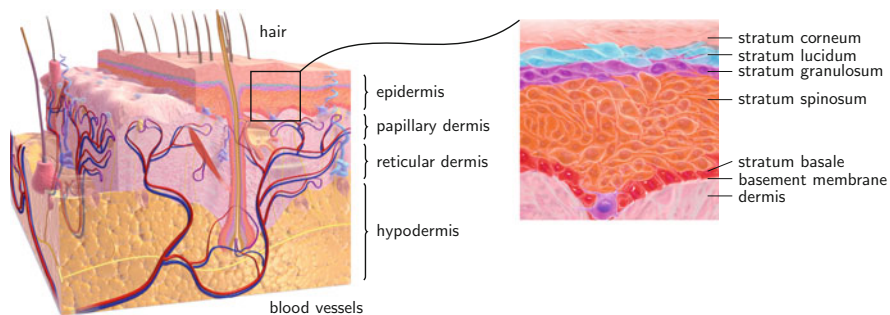

Fig. 1 Representation of the anatomical structure of skin. Skin has functionally different layers that contribute to the overall mechano-biochemical properties of what is the largest organ in the human body. Full thickness skin, left image, generally consists of three layers: the epidermis, dermis, and hypodermis. The epidermis, right image, is the outermost barrier between body and environment, and consists of five sublayers. Adapted from [17]

The dermis is the load-bearing layer in skin and is richly perfused with blood and lymph vessels, and hosts nerve endings. Cutaneous appendages, including sensory receptors, glands, and hair follicles, reside in the dermis which is mostly made up of type I and III collagen. The papillary layer has ridges consisting of thin collagen fibers and provides nutrients to the dermal-epidermal junction. The reticular dermis consists of a dense matrix of collagen bundles and elastin which gives skin its characteristic elastic extensibility.

The hypodermis, the deepest skin layer, primarily serves as a shock absorbing and insulating layer with a location-dependence specialized microstructure. It is located between the dermis and the fascia, which is a thin but strong membrane of connective tissue that encapsulates bones, muscles, and other organs underneath the skin. Fibrous septa running through the hypodermis anchor the dermis to fascial membranes and provide some degree of shear stiffness to the superficial layers of skin. The hypodermis itself contains primarily adipocytes and consists mainly of fat lobules embedded in a loose collagen network.

2.2   Imaging Modalities

In-vivo imaging modalities may generally be categorized by the length scales they resolve and their ability to identify individual pathologies [19]. MRI and US resolve organ and tissue structures at a submillimeter scale [20] and provide a full-thickness representation of skin [21]. High resolution ultrasound [22] and magnetic resonance imaging (MRI) at the organ-level [20] is used to determine layer thicknesses in different body regions and is gaining importance in clinical examinations, due to increased resolution of superficial tissue layers like epidermis and dermis [23]. The echogenicity of individual structures across full-thickness skin is proving useful to diagnose and monitor cysts, scleroderma, and solid, malignant, or inflammatory lesions [24]. It is important to note, however, that individual layers visible in MRI and ultrasound images may differ from medical anatomy. In sonography, and visible in the second row of Fig. 2, skin is often separated into the hyperechoic epidermis, the subepidermal low echogenic band (SLEB) representing the papillary dermis, the dermal echogenic band (DEB) showing reticular dermis, and the mostly hypoechogenic subcutis.

Imaging modalities that visualize skin features down to the cellular level are generally based on the reflective behavior of individual tissue constituents and use either light or lasers as a source for penetrating superficial skin layers [2]. Such non-invasive methods are limited to a penetration depth up to 1000 μm and are therefore primarily used for in vivo characterization of the epidermis and the dermis [28]. Most commonly used methods include reflectance confocal microscopy, optical coherence tomography (OCT), multi-photon microscopy, two-photon fluorescence, and second harmonic generation (SHG).

The characterization of the structural anatomy of the epidermis and dermis -and of the dermal collagen network in particular- is an active field of research [29]. The

High resolution magnetic resonance images of the forehead
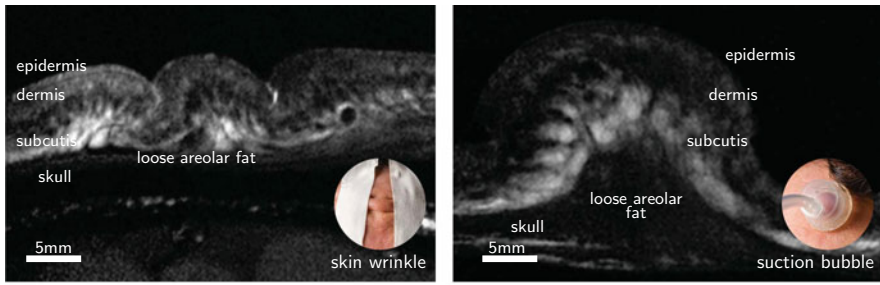
High resolution ultrasound images of three facial regions
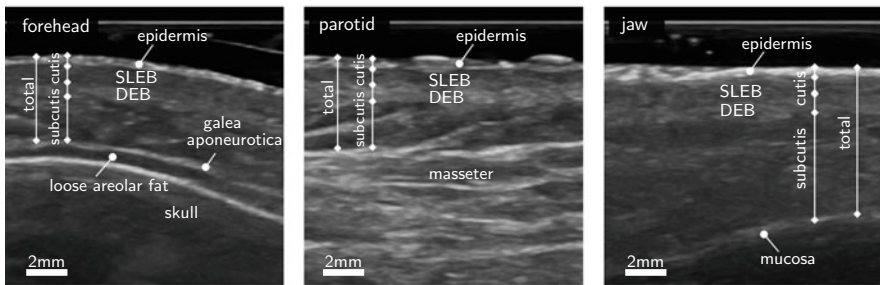
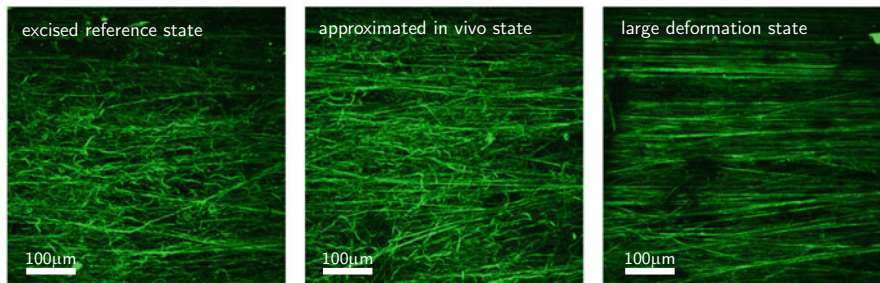**Second harmonic generation images of murine skin collagen**

Fig. 2 High resolution magnetic resonance images of deformed skin in the forehead, top row; high resolution ultrasound images in facial regions, middle row. Each skin layer plays a particular role in providing skin its characteristic extensibility and region-specific mechanical response [25, 26]. Second harmonic generation visualizes the collagen network in excised skin samples: The bottom row shows collagen fibers undulated in the excised reference, and progressively aligned in approximated in vivo, and large deformation states [27]

assembly of collagen fibers into a highly functional network provides skin tissue its characteristic viscoelastic and anisotropic response [30]. The literature reports a rich set of studies investigating microstructure with respect to skin architecture [31, 32], inflammatory and blistering conditions [33], fiber orientation [30, 34], bundle thickness [35], tissue remodeling and skin diseases [36], and cutaneous vasculature [28, 37]. Acute changes of these properties cause structural alterations that may result in reduced extensibility, damage, and patient discomfort [14, 38].

3   Quantification of Mechanical Properties of Skin

Literature provides a rich body of work that investigated the mechanical behavior of skin or individual dermal and subdermal layers [1]. The range of data presented, however, has not led to a complete or consistent description of mechanical skin properties, and the findings continue to show a significant dependence on the testing method used. The biophysical response of skin is just too complex for a single experiment-or the aggregate of experimental data- to fully uncover the mechanisms governing the in vivo relation between local forces and deformations as a function of relevant biomarkers. Thus far, mechanical and biochemical properties are collected at a temporal and spatial scale most relevant to each individual application in medicine, biomechanical engineering, or for cosmetic industry. A comprehensive representation of the hierarchical structure of skin requires investigating the mechanical response across all relevant length and time scales and formulating model equations that allow bridging these scales.

Biomechanical testing methods are generally categorized as either in vivo, in vitro, or ex vivo. They are suitable for the characterization of intact skin or individual layers thereof. Traditionally, skin testing focused on ex-vivo measurements of global force-displacement curves under different loading conditions; recent experiments combine full-field deformation analysis, or tracking of complex 3D deformation of tissue structures, combined with local force measurement. These rich data sets are used to inform skin models of increased complexity which reflect microstructural characteristics. Measurements in many locations across the body illustrate the variation in skin compliance with varying microstructure. One major open question is the rationalization of skin stiffness measurements across several length scales which have provided values ranging from kPa, e.g. [40], to several MPa, e.g. [41].

The most common in vivo and ex vivo measurement methods in skin testing are suction, indentation, and (multiaxial) extension tests (see Fig. 3) and are discussed in the following.

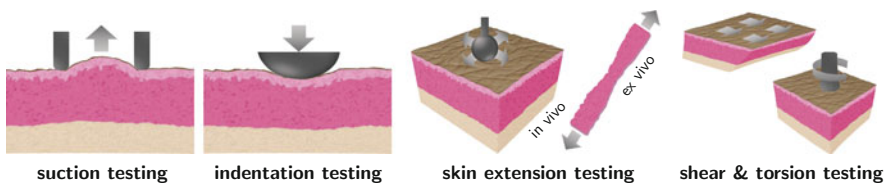suction testing   indentation testing   skin extension testing   shear & torsion testing

Fig. 3 The most common skin testing methods are suction, indentation, extension, shear, and torsion testing. Experimental setups for each method vary significantly across literature. In recent years, full-field in vivo methods have emerged, enabling the characterization of intact skin in its physiological state. Images adapted from [39]

3.1 Suction

Suction measurements are used to determine in vivo and in situ skin properties [1]. The negative pressure draws tissue into the probe opening where an optical system measures bulge height. The resulting relation between pressure and bulge height is directly related to the probe opening size and loading protocol. Most suction devices presented in literature use a 2–8 mm probe opening diameter and apply a negative suction pressure of up to 500mbars [11, 26]. Due to a wide range of possible loading profiles, suction measurements are particularly useful to determine the nonlinear, viscoelastic, and time- and location-dependent behavior of skin [11]. Immediate compliance, elastic recovery, creep, and permanent deformation are represented in corresponding parameters, which are used to quantify the influence of fatigue [42], ageing [43–45], sex [46], and body location [11, 26, 43, 46–49]. Commercially available devices, such as the Cutometer (Cutometer® MPA 580; Courage+Khazaka, Cologne, Germany), come with multiple probe types and a computer interface to prescribe customized loading protocols. Several custom-built devices apply the same principle and might have larger probe openings, like the Aspirator [11, 50], opening shapes [51], or include ultrasound imaging for a visualization of tissue deformation [52]. Although suction data are affected by significant variability, they demonstrate that skin properties vary across the body and are determined by local microstructure. Devices integrating the suction test with ultrasound imaging/optical coherence tomography visualize skin deformation during tissue loading [46, 53]. The results demonstrate that epidermis and dermis are tightly connected and are primarily responsible for skin's local stiffness [6, 53]. Variable probe opening size allows for the recruitment of individual skin layers [11, 54]. Small probe opening size of around 2 mm recruit the most superficial layers of skin, i.e. epidermis and the papillary dermis, while larger opening diameters of about 6–8 mm involve deeper layers, including the reticular dermis as well as the hypodermis or SMAS (superficial musculo aponeurotic system) [26, 53]. Inverse methods, which will be discussed further below, suggest stiffness ratios between superficial and deep skin layers of up to three orders of magnitude difference [11, 53].

Measurements across the body have shown that regions with a loose hypodermis or fatty subcutis, i.e. jaw, cheek, and neck, tend to respond more elastically [26, 44] than regions with a dense dermal matrix that connects the deep fascia with superficial skin layers, i.e. hands, forearm, and forehead [11, 44]. In fact, the face is a representative region of the body for which functionally driven microstructure characteristics can be linked with differences in skin mechanics, with the forehead being stiffest, followed by the parotid region and the jaw [26].

Suction experiments have well-known limitations. First, the mechanical analysis is based on the simplifying assumption that skin is isotropic. In fact, given the circular opening of typical suction probes, it is impossible to characterize the anisotropic properties of skin from these tests. Second, the measured response is dominated by the characteristics of the superficial layers, while the influence

of deeper layer diminishes with their distance from the surface, in particular for small probe openings. Third, the repeatability of suction measurements depends on accurate probe handling, especially for hand-held devices such as a the Cutometer. Repeated probe placement-including proper alignment of probe and skin and control of contact pressure are paramount to ensure reliable measurement results [55, 56]. The development of an experimental setup that minimizes movement between probe and skin surface and maintains constant contact pressure improved measurement results for multiple repetitions per measurement site and probe diameter size [11, 26].

3.2   Indentation

Indentation is another widely used in vivo testing method as it enables a non-invasive measurement. Unlike the suction method, indentation testing is restricted to flat body regions, such as the volar forearm or the calf [57, 58]. Direct mechanical interpretation of indentation tests is restricted to a linear analysis of the quasi-static or linear viscoelastic properties of skin. Combination of nonlinear analysis and an inverse scheme are necessary to inform more complex models [59]. A major challenge in indentation of soft biological tissues is the reliable identification of the initial contact point between indenter tip and skin surface during loading as well as the assessment of adhesion effects during unloading. Lastly, in-vivo indentation tests do not allow for a quantification of the anisotropic tissue response, since the unidirectional registration of force and displacement does not allow to detect a direction-dependent tissue response.

Indentation tests have shown that volar forearm skin softens with age and progressively loses elasticity, most likely due to microstructural changes in the dermis and hypodermis [58, 60, 61]. The same experimental setup was used to measure the dynamic response of superficial skin at an indentation depth of $200 \pm 3 \, \mu m$ in a range of 10–60 Hz. At these low indentation depths, skin stiffness and viscosity were found to be frequency independent [57], which may suggest that the dermal matrix is not activated at a relevant length scale.

A more recent study investigated stiffness and viscosity in reconstructed skin [62]. A series of quasi-static, force-controlled indentation / creep experiments (including a hold time of 100 s after reaching a maximum indentation force of 0.5 mN) were conducted to assess differences in tissue properties at critical stages during the in vitro reconstruction of skin. It was found that skin substitutes stiffen significantly once keratinocytes are seeded on top of the reconstructed dermis to form an epidermal layer. This finding is very insightful in view of the generally accepted claim that skin stiffness is primarily originating from the dermis.

Atomic force microscopy (AFM) is an indentation-based measurement method and has been used to quantify the impact of hydration on the mechanical response of the stratum corneum and epidermis [60, 61]. Indentation depths of up to 200 nm are three orders of magnitude smaller than the previously described indentation

tests and therefore capture the mechanical response at a much smaller length scale. General observations from studies using AFM are that scar tissue is generally stiffer than healthy skin [63] and that the Young's modulus of stratum corneum is roughly twice as high as for the epidermis [64]. Latter study reported stiffness values in the range of 1–2 MPa in comparison to values reported for "skin" (varying due to age) between 5–10 kPa by [40, 57, 58]. Indentation experiments thus provide compelling evidence of the length scale influence on the mechanical properties of skin.

3.3 Skin Extension Tests

Skin extension tests have been used to characterize ex vivo mechanical properties of skin and individual layers thereof. Unlike suction and indentation, extension testing allows investigating the anisotropic response of skin as it relates to the Langer lines distributed across the body [65, 66]. Further, it is used to characterize the time and history dependent behavior of skin through monotonic and cyclic creep and relaxation experiments, e.g. [67].

In most studies, samples are cut from excised skin and clamped inside a uniaxial or multiaxial loading rig [41]. Inevitably, mechanical properties change upon excision and strongly depend on storage duration, storage conditions, and temperature. Sample preparation, often in the form of removing the epidermis as well as adipose tissue to isolate the dermal layer, represents a major interference with the physiological state of alive skin tissue [41, 68]. In fact, cutting away or peeling off of individual layers might damage the structural connections between individual layers. Extraction of skin from the body leads to the loss of in vivo multiaxial pre-tension, so that the peculiar in vivo tensioned configuration of collagen and elastin networks is lost thus leading to unphysiological stress-strain measurements.

Most skin extension studies interpret the experimental data on the basis of linear elasticity theory, extracting the slope of the linear regime of the overall nonlinear, J-shaped force-displacement curve [41, 69]. The most frequently reported parameters from uni- or multiaxial measurements are the ultimate tensile strength and the elastic modulus of the dermis [41]. Fewer studies derive non-linear model parameters through a finite element based inverse analysis [70]. Finite strain models usually require an inverse scheme to identify model parameters that match prediction and observation. Time-independent models are typically associated with quasi-static loading conditions, in the form of slow loading rates.

Flynn et al. [71] presented a setup to measure the three-dimensional force-displacement response of in vivo skin in multiple directions. The system captures the nonlinear and viscoelastic skin behavior at different measurement sites and allows to determine the anisotropic properties of skin by gradually changing the loading direction. As one of the few studies found in literature, the resulting data set is used to fit an anisotropic material model [72].

Recent studies were able to visualize local microstructural tissue deformation, often using Two-Photon Excited Fluorescence or second harmonic generation (SHG), while gradually loading the sample [29, 30]. Bancelin et al. [30] show that mice dermal collagen matrix undergoes three characteristic mechanisms in uniaxial tension experiments: (i) realignment of collagen fibers along the principal direction of stretch during the early loading phase; noticeable levels of stretch at low loads and low stiffness, (ii) tissue stiffening due to the recruitment of load bearing fibers aligned with the primary direction of loading, and (iii) a linear regime in the stress strain curve due to intra-and interfibrillar sliding in collagen fibers. Tissue loaded beyond its fracture point leads to widespread breakage of fibrils and their immediate recoil [70]. The distribution of fiber orientation is strongly coupled to the stiffness regime of the tissue and highlights the relevance of properly accounting for in vivo stress.

Pensalfini et al. [29] analyzed excised mice skin samples including a previously induced excisional wound. Uniaxial tension tests were performed to visualize the heterogeneity within the strain field of the wound region [29]. It was observed that skin tissue around the wound can be divided into mechanically distinct regions displaying microstructurally motivated stretch patterns. While skin in the core of the wound showed little extensibility, a highly compliant zone next to the wound accommodates the majority of tissue deformation. Concomitant histological analysis and SHG imaging demonstrated that the presence of the compliant region avoids the recruitment of newly deposited collagen fibers in the early phase of healing.

3.4   Other Testing Methods

Other, less common, skin testing methods include torsion testing, the bulge method, and static and dynamic shear load methods. Torsion experiments were among the earliest applied to characterize the in vivo response of skin [73, 74] and inspired the development of suction devices in later years. Bulge tests performed by [75] provided information on the macroscopic biaxial response of skin and reported stiffness values of around 11 MPa for the linear regime of the stress-strain curve; strikingly, a tenfold increase in skin stiffness was observed from the toe region to the linear regime with an average transition stretch value of 1.1. And lastly, full thickness shear measurements indicated a large variation of around 100% in the shear modulus depending on depth [76]. Epidermis was found to be almost two times stiffer than dermis in these large amplitude shear oscillatory tests, which is in contrast with the common claim that the mechanical response of the epidermis has negligible influence [53].

3.5 Summary

The review of experimental data on in vivo and ex vivo human skin highlights the complex nature of skin biophysics. Its mechanical behavior is nonlinear, viscoelastic, and anisotropic. Significant differences between in vivo and ex vivo measurements exist, and they might be linked with the level of in vivo tension of skin, which is difficult to quantify or reproduce in ex vivo settings. This poses a significant limitation, as most computational models assume a stress-free initial state. Knowledge of the physiological loading state of skin is relevant also for the assessment of the mechanical biocompatibility of tissue engineered skin substitutes and their scaffolds [27, 77].

4   Constitutive Modeling

Modeling of the mechanical behavior of skin has been the objective of biomechanics studies for several decades and remains an active field of research [1]. Given the highly complex mechanical response of individual skin structures as well as the interaction at the interface of sublayers, skin modeling requires not only the formulation of a material model, but a corresponding representation of skin anatomy as well. In most studies reported in literature, skin is homogenized into a single layer including epidermis, dermis, and potentially even hypodermis. Fewer studies apply a multilayered representation and differentiate between epidermis, papillary and reticular layer of dermis, and hypodermis or SMAS [11, 78].

The interpretation of experimental data using inverse analysis depends on the chosen mathematical description of the stress-strain relation, as well as on the anatomic reconstruction. Very often, application specific skin models are developed, such as e.g. for the simulation of skin response to cosmetic products [79], the role of skin in facial expressions or mastication [6, 7], or the prediction of scar tissue formation due to suture tension [80]. Chapter "Constitutive Modelling of Skin Mechanics" reviews constitutive model formulations for skin. In this section, we will briefly discuss the different type of material model equations, their parameters and how they relate to the inverse analysis of experimental data.

Early models focused on integrative strategies to represent the mechanical response of individual constituents of the extracellular matrix [81]. Such collagen-based models represent the degree of fibers undulation and its progressive reduction as the matrix deforms. Evidence based implementation of these models requires a thorough characterization of the microstructure for each sublayer of the skin. For most specific applications such level of detail is unknown, and experiments may not provide the information relevant to respective length scales and structures. Hence, most material models proposed in literature generally homogenize the tissues response and aim at reproducing the experimentally observed stress-strain curves [12]. Next to physically motivated formulations for structural models, commonly

used constitutive models are often based on phenomenological parameters. A common assumption is that skin behaves as incompressible, although no experimental evidence was reported on this property. Corresponding measurements are needed, since recent findings indicates that interstitial fluid motion might lead to significant volume changes in soft collagenous tissues [82]. The most relevant model equations applied for the analysis of experiments on skin are listed below. Many of these material models include a large number of parameters which cannot be measured directly and require an inverse identification scheme, as will be discussed in the following section. Table 1 summarizes material models frequently found in skin literature.

5   Parameter Identification Methods

Constitutive model parameter identification is a broad field of research and a variety of optimization schemes were proposed in the literature. Within the specific context of skin modeling, there are a few popular approaches that have proven useful for the identification of potentially large parameter sets. The following section provides a summary of these optimization schemes specific to skin models.

On the most abstract level, the choice of the appropriate optimization scheme depends on the availability of an analytical expression for the relation between stress and strain of the experiment providing the data. If skin is treated as a linear or nonlinear solid, such analytical solutions exists for all commonly applied loading conditions including uniaxial and planar biaxial tension/compression experiments [97]. Model parameters are then identified by a least-squares fit analysis which minimizes the sum of squared differences between the experimentally observed force-deformation (or stress-strain) curve and corresponding model predictions. These tests are usually performed on ex vivo or in vitro skin tissue samples. In vivo skin tissue measurements usually involve more complex deformation patterns for which no analytical expression exists. In these cases, the relation between material constants and experimental data is implicit and requires a numerical approach to determine a set of material parameters that minimizes the difference between the observed and predicted tissue response [11].

Optimization schemes minimize an objective function which may or may not explicitly depend on the model parameters. Two general classes of optimization algorithms exist: In one case, algorithms require an analytical or numerical evaluation of the objective function's gradients in the model parameter space [98]; the second class are derivative-free methods and include so called simplex algorithms [99].

Derivative-free methods have proven most useful in skin mechanics because they provide robust schemes for multidimensional parameter spaces [97]. Most skin models discussed in chapter "Constitutive Modelling of Skin Mechanics" have a large number of model parameters and assume a geometrically and structurally complex representation of skin, and therefore require the use of heuristic search

Table 1 Common constitutive models, main model features, number of parameters m, and accompanying experiments to identify model parameters

Model	Main features	m	Accompanying experiments
Neo–Hookean, Mooney–Rivlin, and Ogden (1)	Isotropic, hyperelastic	2–6	In vivo suction [53, 83]; in vivo indentation [59]; in vivo multiaxial extension [71, 72, 84]
Tong and Fung (2)	Anisotropic, nonlinear	13	Ex vivo uni- and biaxial tension and relaxation [85, 86]; in vivo multiaxial extension [87]
Lanir (3)	Anisotropic, viscoelastic	>11	Ex vivo uni- and biaxial tension and relaxation [85, 86]; in vivo uniaxial tension [88]
Weiss (4)	Transversely isotropic, hyperelastic	14	Ex vivo tensile tests [89]
Bischoff–Arruda–Grosh (5)	Anisotropic, viscoelastic	15	Ex vivo biaxial tension and relaxation [85, 86]
Rubin–Bodner (6)	Anisotropic, elastic-viscoplasticity	14	Ex vivo biaxial tension and relaxation [85, 86]; in vivo suction [11, 47]
Limbert (7)	Transversely isotropic, viscoelastic	23	Ex vivo biaxial tension and relaxation [85, 86]
Flynn–Rubin–Nielsen (8)	Discrete fiber model	11	Ex vivo biaxial tension [85, 86] ex vivo uniaxial tension

Labels in model column: 1—Rivlin [90], Ogden [91]; 2—Tong and Fung [92]; 3—Lanir [81]; 4—Weiss et al. [93]; 5—Bischoff et al. [94]; 6—Rubin and Bodner [67]; 7—Limbert [95]; 8—Flynn et al. [96]
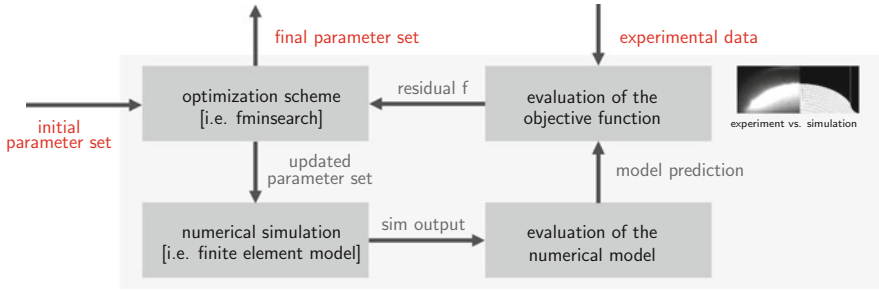
Fig. 4 Common implementation of inverse analysis algorithms (e.g. the *fminsearch* algorithm) for skin parameter identification schemes. The optimization scheme iteratively determines a model parameter set that minimizes the error between experimental data and the associated numerical simulation. During each iteration, a finite element simulation is necessary to predict the model response based on the updated parameter set

methods that are more likely to find a minimum of the objective function. Several implementations of derivative-free optimization schemes exist, and the fminsearch function in Matlab (The MathWorks Inc., Natick, Massachusetts, US) is widely used throughout skin literature. The fminsearch function uses the Nelder-Mead simplex algorithm [100, 101]: in an n-dimensional parameter space, the algorithm maintains $n + 1$ test points arranged as a simplex. The behavior of the objective function measured at each test point is used to extrapolate new test points and to replace those, that provide the worst response. Different strategies exist to update the test points and the algorithm will stop if the sample standard deviation of the objective function falls below a prescribed tolerance. As shown in Fig. 4, an initial parameter set is iteratively updated through an optimization algorithm, i.e. the *fminsearch* function, to minimize the error between experimental data and the associated numerical simulation. During each iteration, a finite element simulation is necessary to determine the model response based on the updated parameter set. The number of parameters, the number of simulations necessary per iteration, and the degree of coupling between parameters determine the required computation time and the uniqueness of the final parameter set.

Several groups working on skin mechanics have developed specialized optimization schemes, that range from a simultaneous fit of all model parameters to a sequential determination for individual layers and loading conditions. Weickenmeier et al. [11] performed suction experiments with varying probe opening diameters to recruit superficial and deeper skin layers individually. An initial sensitivity analysis of the accompanying multi-layered finite element skin model revealed strong coupling between material parameters as well as a significant influence of individual layers on the deformation field for different probe opening diameters. Sequential fitting of individual layers resulted in a stiffness ratio between the superficial and deep layer corresponding to two orders of magnitude difference [47]. The simultaneous fitting of superficial and deep material parameters using four different loading conditions to capture the instantaneous and transient response of

skin, provided more homogeneous results [11] which seem more reasonable in view of previously reported ex-vivo mechanical analysis of dermal tissue and SMAS [67].

Hendrik and co-authors presented a series of suction based skin experiments and corresponding model parameter fits [52, 53, 102]. While initially working with a single layer model [53, 102] and later extending skin to a two-layer model, Hendrik et al. used a constrained nonlinear optimization function based on Sequential Quadratic Programming (SQP), to determine all material parameters in parallel. Their two-layer model predicted three orders of magnitude difference between superficial and deeper layers. This outcome is motivated by the finite element model implementation and the weight of individual measurement curves on the overall cost function.

Flynn and co-authors' in vivo multi-axial skin loading device requires a finite element model for data analysis [96]. In a process similar to previously presented schemes, model parameters of a single layer skin model-including in vivo stress-are determined based on a nonlinear least-squares curve fitting algorithm. Based on the trust region method, a set of initial parameters is iteratively improved to minimize the error between experiment and model, while running a finite element simulation at each iteration to evaluate the model-based tissue response. Two different models were tested: an isotropic Ogden model [91] and the anisotropic Tong and Fung model [92]. The total number of parameters fit simultaneously were 4, 6, and 8, depending on the model formulation. The error function was calculated as the sum over all measurement directions and the in vivo stress level was used to represent the anisotropy of the tissue response. Jor et al. [103], using the same experimental setup, aimed at fitting a microstructurally motivated constitutive relation with 7 parameters.

With the emergence of experimental methods combining force measurements with video imaging of the accompanying deformation field, more elaborate and localized inversion schemes are presented in literature. The quantitative assessment of the heterogeneity of the deformation fields allows to determine material parameters at a local scale and are based on so called full-field methods. Avril et al. [104] presents an overview of corresponding inverse analysis schemes. In comparison to the above-mentioned methods, the new approaches solve the nonlinear elasticity equations based on the pointwise experimentally observed deformation field. This procedure allows using derivative-based methods, which are more reliable in that they are more likely to provide a global minimum. The associated increase in computational cost to evaluate the derivative of the objective function is often linked with the requirement of increased computational power.

6 Outlook

Skin is a complex biological system that is characterized by an intricate interplay between individual tissue layer and ECM components at different length scales. The interaction of the different components of the extracellular matrix and the different

layers depends on the state of deformation imposed to the skin, with different mechanisms influencing in-plane tension, in-plane or out-of-plane shear, and skin bending. Although a large number of mechanical tests has been conducted, our understanding of full-thickness skin behavior remains incomplete. New integrative testing methods, i.e. simultaneous visualization of tissue and microstructure kinematics during mechanical response to a wide range of loading conditions, as well as the analysis of skin properties in relation to observable microstructural parameters, represent promising approaches to improve our understanding of skin mechanics.

The range of mechanical properties reported in literature and the dependence of the mechanical response on the testing method used continues to represent a major challenge in determining a universal description of skin mechanics. In this context, a specific problem is represented by the mismatch in stiffness reported for different tissue length scales interrogated in the different experiments. The quantification of in vivo stress represents another critical question in skin mechanics: As most computational models assume a test specific stress-free initial state, existing parameter sets proposed in literature are likely to grossly misrepresent the actual in-vivo response of skin tissue.

Anatomy based skin models used in parameter identification schemes will become more reliable as we continue to improve our understanding of the relation between local microstructure and mechanical response. Essential input will be obtained through in vivo and ex vivo application of full field methods and the associated model parameter identification procedures. The systematic combination of computer-based modeling and multiscale experimental data acquisition will facilitate the development of biomechanical and mechanobiological models with enhanced predictive capabilities. Improved understanding of skin biomechanics will allow future research to focus on highly relevant medical questions, such as impaired wound healing, skin suturing, reconstructive surgery, skin tissue engineering, as well as diagnosis and monitoring of specific skin diseases.

References

1. Jor JWY, Parker MD, Taberner AJ, Nash MP, Nielsen PMF (2013) Computational and experimental characterization of skin mechanics: identifying current challenges and future directions. Wiley Interdiscip Rev Syst Biol Med 5(5):539–556
2. Hani AFM (2014) Surface imaging for biomedical applications. CRC, Boca Raton
3. Forbes SJ, Rosenthal N (2014) Preparing the ground for tissue regeneration: from mechanism to therapy. Nat Med 20(8):857
4. Murphy PS, Evans GRD (2012) Advances in wound healing: a review of current wound healing products. Plast Surg Int 2012:8. https://doi.org/10.1155/2012/190436
5. Rowan MP, Cancio LC, Eric A, Burmeister DM, Rose LF, Natesan S, Chan RK, Christy RJ, Chung KK (2015) Burn wound healing and treatment: review and advancements. Crit Care 19(1):243
6. Weickenmeier J, Wu R, Lecomte-Grosbras P, Witz J-F, Brieu M, Winklhofer S, Andreisek G, Mazza E (2014) Experimental characterization and simulation of layer interaction in facial soft tissues. In: Intrnational symposium on biomedical simulation. Springer, Cham, pp 233–241

7. Limbert G, Kuhl E (2018) On skin microrelief and the emergence of expression micro-wrinkles. Soft Matter 14(8):1292–1300

8. Buganza Tepole A, Joseph Ploch C, Wong J, Gosain AK, Kuhl E (2011) Growing skin: a computational model for skin expansion in reconstructive surgery. J Mech Phys Solids 59(10):2177–2190

9. Zöllner AM, Buganza Tepole A, Gosain AK, Kuhl E (2012) Growing skin: tissue expansion in pediatric forehead reconstruction. Biomech Model Mechanobiol 11(6):855–867

10. Lee T, Turin SY, Gosain AK, Tepole AB (2018) Multi-view stereo in the operating room allows prediction of healing complications in a patient-specific model of reconstructive surgery. J Biomech 74:202–206

11. Weickenmeier J, Jabareen M, Mazza E (2015) Suction based mechanical characterization of superficial facial soft tissues. J Biomech 48(16):4279–4286

12. Limbert G (2017) Mathematical and computational modelling of skin biophysics: a review. Phil Trans R Soc A 473(2203):20170257

13. Oomens C (2017) Mechanical behaviour of skin: the struggle for the right testing method. In: Avril S, Evans S (eds) Material parameter identification and inverse problems in soft tissue biomechanics. Springer, Cham, pp 119–132

14. Koehler MJ, Lange-Asschenfeldt S, Kaatz M (2011) Non-invasive imaging techniques in the diagnosis of skin diseases. Expert Opin Med Diagn 5(5):425–440

15. Wong R, Geyer S, Weninger W, Guimberteau J-C, Wong JK (2016) The dynamic anatomy and patterning of skin. Exp Dermatol 25(2):92–98

16. Weissleder R (2011) A clearer vision for in vivo imaging. Nat Biotechnol 19:316–317

17. Blausen Medical (2014) Dermal circulation. WikiJ Med 1(2):10

18. LaTrenta G (2004) Atlas of aesthetic face and neck surgery. W.B. Saunders, Philadelphia

19. Aspres N, Egerton IB, Lim AC, Shumack SP (2003) Imaging of Skin. Australas J Dermatol 44(1):19–27

20. Mirrashed F, Sharp JC (2004) In vivo morphological characterisation of skin by MRI micro-imaging methods. Skin Res Technol 10(3):149–160

21. Barral JK, Bangerter NK, Hu BS, Nishimura DG (2010) In vivo high-resolution magnetic resonance skin imaging at 1.5 T and 3 T. Magn Reson Med 63(3):790–796

22. Van Mulder TJS, de Koeijer M, Theeten H, Willems D, Van Damme P, Demolder M, De Meyer GRY, Beyers KCL, Vankerckhoven V (2017) High frequency ultrasound to assess skin thickness in healthy adults. Vaccine 35(14):1810–1815

23. Kleinerman R, Whang TB, Bard RL, Marmur ES (2012) Ultrasound in dermatology: principles and applications. J Am Acad Dermatol 67(3):478–487

24. Wortsman, Ximena, Jacobo Wortsman, Laura Carreño, Claudia Morales, Ivo Sazunic, Gregor B. E. Jemec 2013 Sonographic anatomy of the skin, appendages, and adjacent structures. Springer, New York. https://link.springer.com/chapter/10.1007/978-1-4614-7184-4_2. Accessed 29 Apr 2018

25. Weickenmeier J (2015) Investigation of the mechanical behavior of facial soft tissues. ETH Zurich, Zurich

26. Pensalfini M, Weickenmeier J, Rominger MB, Santoprete R, Distler O, Mazza E (2018) Location-specific mechanical response and morphology of facial soft tissues. J Mech Behav Biomed Mater 78:108–115

27. Pensalfini M, Ehret AE, Stüdeli S, Marino D, Kaech A, Reichmann E, Mazza E (2017) Factors affecting the mechanical behavior of collagen hydrogels for skin tissue engineering. J Mech Behav Biomed Mater 69:85–97

28. Chen Z, Rank E, Meiburger KM, Sinz C, Hodul A, Zhang E, Hoover E et al (2017) Non-invasive multimodal optical coherence and photoacoustic tomography for human skin imaging. Sci Rep 7(1):17975

29. Pensalfini M, Haertel E, Hopf R, Wietecha M, Werner S, Mazza E (2018) The mechanical fingerprint of murine excisional wounds. Acta Biomater 65:226–236

30. Bancelin S, Lynch B, Bonod-Bidaud C, Ducourthial G, Psilodimitrakopoulos S, Dokládal P, Allain J-M, Schanne-Klein M-C, Ruggiero F (2015) Ex vivo multiscale quantitation of skin

biomechanics in wild-type and genetically-modified mice using multiphoton microscopy. Sci Rep 5(1):17635–17635

31. Yasui T, Takahashi Y, Ito M, Fukushima S, Araki T (2009) Ex vivo and in vivo second-harmonic-generation imaging of dermal collagen fiber in skin: comparison of imaging characteristics between mode-locked Cr:forsterite and Ti:sapphire lasers. Appl Opt 48(10):D88–D95

32. Adabi S, Hosseinzadeh M, Noei S, Conforto S, Daveluy S, Clayton A, Mehregan D, Nasiriavanaki M (2017) Universal in vivo textural model for human skin based on optical coherence tomograms. Sci Rep 7(1):17912

33. Avanaki MR, Hojjatoleslami A, Sira M, Schofield JB, Jones CA, Podoleanu AG (2013) Investigation of basal cell carcinoma using dynamic focus optical coherence tomography. Appl Opt 52(10):2116–2124

34. Yasui T, Tohno Y, Araki T (2004) Characterization of collagen orientation in human dermis by two-dimensional second-harmonic-generation polarimetry. J Biomed Opt 9(2):259–264

35. Chen X, Nadiarynkh O, Plotnikov SV, Campagnola PJ (2012) Second harmonic generation microscopy for quantitative analysis of collagen fibrillar structure. Nat Protoc 7(4):654–669

36. Chen S-Y, Chen S-U, Hai-Yin W, Lee W-J, Liao Y-H, Sun C-K (2010) In vivo virtual biopsy of human skin by using noninvasive higher harmonic generation microscopy. IEEE J Sel Top Quantum Electron 13(3):478–492

37. Shirshin EA, Gurfinkel YI, Priezzhev AV, Fadeev VV, Lademann J, Darvin ME (2017) Two-photon autofluorescence lifetime imaging of human skin papillary dermis in vivo: assessment of blood capillaries and structural proteins localization. Sci Rep 7(1):1171

38. Koehler MJ, Hahn S, Preller A, Elsner P, Ziemer M, Bauer A, König K, Bückle R, Fluhr JW, Kaatz M (2008) Morphological skin ageing criteria by multiphoton laser scanning tomography: non-invasive in vivo scoring of the dermal fibre network. Exp Dermatol 17(6):519–523

39. Pond D, McBride AT, Davids LM, Reddy BD, Limbert G (2018) Microstructurally-based constitutive modelling of the skin – linking intrinsic ageing to microstructural parameters. J Theor Biol 444:108–123

40. Achterberg VF, Buscemi L, Diekmann H, Smith-Clerc J, Schwengler H, Meister J-J, Wenck H, Gallinat S, Hinz B (2014) The nano-scale mechanical properties of the extracellular matrix regulate dermal fibroblast function. J Investig Dermatol 134(7):1862–1872

41. Annaidh AN, Bruyère K, Destrade M, Gilchrist MD, Otténio M (2012) Characterization of the anisotropic mechanical properties of excised human skin. J Mech Behav Biomed Mater 5(1):139–148

42. Dobrev H (2005) Application of Cutometer area parameters for the study of human skin fatigue. Skin Res Technol 11(2):120–122

43. Luebbberding S, Krueger N, Kerscher M (2014) Mechanical properties of human skin in vivo: a comparative evaluation in 300 men and women. Skin Res Technol 20(2):127–135

44. Krueger N, Luebbberding S, Oltmer M, Streker M, Kerscher M (2011) Age-related changes in skin mechanical properties: a quantitative evaluation of 120 female subjects. Skin Res Technol 17(2):141–148

45. Ryu HS, Joo YH, Kim SO, Park KC, Youn SW (2008) Influence of age and regional differences on skin elasticity as measured by the Cutometer. Skin Res Technol 14(3):354–358

46. Diridollou S, Black D, Lagarde JM, Gall Y, Berson M, Vabre V, Patat F, Vaillant L (2000) Sex-and site-dependent variations in the thickness and mechanical properties of human skin in vivo. Int J Cosmet Sci 22(6):421–435

47. Barbarino GG, Jabareen M, Mazza E (2011) Experimental and numerical study on the mechanical behavior of the superficial layers of the face. Skin Res Technol 17(4):434–444

48. Luboz V, Promayon E, Payan Y (2014) Soft tissue finite element modeling and calibration of the material properties in the context of computer-assisted medical interventions. Ann Biomed Eng 42(11):2369–2378

49. Kim MA, Kim EJ, Lee HK (2018) Use of SkinFibrometer® to measure skin elasticity and its correlation with Cutometer® and DUB® Skinscanner. Skin Res Technol 24(3):466–471
50. Nava A, Mazza E, Kleinermann F, Avis NJ, McClure J (2003) Determination of the mechanical properties of soft human tissues through aspiration experiments. In: International Conference on Medical Image Computing and Computer-Assisted Intervention. Springer, New York, pp 222–229
51. Iivarinen JT, Korhonen RK, Julkunen P, Jurvelin JS (2013) Experimental and computational analysis of soft tissuemechanical response under negative pressure in forearm. Skin Res Technol 19(1):356–365
52. Hendriks F, Brokken D, Oomens C, Bader D, Baaijens F (2006) The relative contributions of different skin layers to the mechanical behavior of human skin in vivo using suction experiments. Med Eng Phys 28(3):259–266
53. Hendriks F, Brokken D, Van Eemeren J, Oomens C, Baaijens F, Horsten J (2003) A numerical-experimental method to characterize the non-linear mechanical behaviour of human skin. Skin Res Technol 9(3):274–283
54. Schlangen LJM, Brokken D, Van Kemenade PM (2003) Correlations betwen small aperture skin suction parameter- statistical analysis and mechanical model. Skin Res Technol 9(2):122–130
55. Bonaparte JP, Chung J (2014) The effect of probe placement on inter-trial variability when using the Cutometer MPA 580. J Med Eng Technol 38(2):85–89
56. Bonaparte JP, Ellis DA, Chung J (2013) The effect of probe to skin contact force on Cutometer MPA 580 measurements. J Med Eng Technol 37(3):208–212
57. Boyer G, Laquièze L, Le Bot A, Laquièze S, Zahouani H (2009) Dynamic indentation on human skin in vivo: ageing effects. Skin Res Technol 15(1):55–67
58. Pailler-Mattei C, Debret R, Vargiolu R, Sommer P, Zahouani H (2013) In vivo skin biophysical behaviour and surface topography as a function of ageing. J Mech Behav Biomed Mater 28:474–483
59. Delalleau A, Josse G, Lagarde J-M, Zahouani H, Bergheau J-M (2006) Characterization of the mechanical properties of skin by inverse analysis combined with the indentation test. J Biomech 39(9):1603–1610
60. Zahouani H, Vargiolu R, Boyer G, Pailler-Mattéi C, Laquièze L, Mavon A (2009) Friction noise of human skin in vivo. Wear 267(2):1274–1280
61. Zahouani H, Boyer G, Pailler-Mattéi C, Ben Tkaya M, Vargiolu R (2011) Effect of human ageing on skin rheology and tribology. Wear 271:2364–2369
62. Tupin S, Molimard J, Cenizo V, Hoc T, Sohm B, Zahouani H (2016) Multiscale approach to characterize mechanical properties of tissue engineered skin. Ann Biomed Eng 44(9):2851–2862
63. Grant CA, Twigg PC, Tobin DJ (2012) Static and dynamic nanomechanical properties of human skin tissue using atomic force microscopy: effect of scarring in the upper dermis. Acta Biomater 8(11):4123–4129
64. Geerligs M, van Breemen L, Peters GWM, Ackermans PAJ, Baaijens FF, Oomens C (2011) In vitro indentation to determine the mechanical properties of epidermis. J Biomech 44(6):1176–1181
65. Langer K (1862) Zur Anatomie und Physiologie der Haut – II – Die spannung der cutis. Sitzungsberchte der Mathematisch-naturwissenschaftlicher Classe der. Kaiserlichen Akademie der Wissenschaften 45:133
66. Langer K (1978) On the anatomy and physiology of the skin: I. The cleavability of the cutis. Br J Plast Surg 31(1):3–8
67. Rubin MB, Bodner SR (2002) A three-dimensional nonlinear model for dissipative response of soft tissue. Int J Solids Struct 39(19):5081–5099
68. Har-Shai Y, Bodner SR, Egozy-Golan D, Lindenbaum ES, Ben-Izhak O, Mitz V, Hirshowitz B (1996) Mechanical properties and microstructure of the superficial musculoaponeurotic system. Plast Reconstr Surg 98(1):59–70

69. Shergold OA, Fleck NA, Radford D (2006) The uniaxial stress versus strain response of pig skin and silicone rubber at low and high strain rates. Int J Impact Eng 32(9):1384–1402
70. Yang W, Sherman VR, Gludovatz B, Schaible E, Stewart P, Ritchie RO, Meyers MA (2015) On the tear resistance of skin. Nat Commun 6:6649
71. Flynn C, Taberner AJ, Nielsen PMF (2011) Measurement of the force–displacement response of in vivo human skin under a rich set of deformations. Med Eng Phys 33(5):610–619
72. Flynn C, Taberner A, Nielsen P (2011) Modeling the mechanical response of in vivo human skin under a rich set of deformations. Ann Biomed Eng 39(7):1935–1946
73. Sanders R (1973) Torsional elasticity of human skin in vivo. Pflügers Archiv Eur J Phys 342(3):255–260
74. Escoffier C, de Rigal J, Rochefort A, Vasselet R, Lévêque J-L, Agache PG (1989) Age-related mechanical properties of human skin- an in vivo study. J Investig Dermatol 93(3):353–357
75. Tonge TK, Atlan LS, Voo LM, Nguyen TD (2013) Full-field bulge test for planar anisotropic tissues: part I–experimental methods applied to human skin tissue. Acta Biomater 9(4):5913–5925
76. Lamers E, T.H.S v K, F.P.T B, G.W.M P, C.W.J O (2013) Large amplitude oscillatory shear properties of human skin. J Mech Behav Biomed Mater 28:462–470
77. Mazza E, Ehret AE (2015) Mechanical biocompatibility of highly deformable biomedical materials. J Mech Behav Biomed Mater 48:100–124
78. Leyva-Mendivil MF, Page A, Bressloff NW, Limbert G (2015) A mechanistic insight into the mechanical role of the stratum corneum during stretching and compression of the skin. J Mech Behav Biomed Mater 49:197–219
79. Boissieux L, Kiss G, Thalmann NM, Kalra P 2000 Simulation of skin aging and wrinkles with cosmetics insight.https://link.springer.com/chapter/10.1007/978-3-7091-6344-3_2. Accessed 8 Apr 2018
80. Lee T, Vaca EE, Ledwon JK, Bae H, Topczewska JM, Turin SY, Kuhl E, Gosain AK, Buganza A (2018) Improving tissue expansion protocols through computational modeling. J Mech Behav Biomed Mater 82:224–234
81. Lanir Y (1983) Constitutive equations for fibrous connective tissues. J Biomech 16(1):1–12
82. Ehret AE, Bircher K, Stracuzzi A, Marina V, Zündel M, Mazza E (2017) Inverse poroelasticity as a fundamental mechanism in biomechanics and mechanobiology. Nat Commun 8(1):1002
83. Delalleau A, Josse G, Lagarde J-M, Zahouani H, Bergheau J-M (2008) A nonlinear elastic behavior to identify the mechanical parameters of human skin in vivo. Skin Res Technol 14(2):152–164
84. Evans SL, Holt CA (2009) Measuring the mechanical properties of human skin in vivo using digital image correlation and finite element modelling. J Strain Anal Eng Des 44(5):337–345
85. Lanir Y, Fung YC (1974) Two-dimensional mechanical properties of rabbit skin—II. Experimental results. J Biomech 7(2):171–174
86. Lanir Y, Fung YC (1974) Two-dimensional mechanical properties of rabbit skin—I. Experimental system. J Biomech 7(1):29–34
87. Kvistedal YA, Nielsen PMF (2009) Estimating material parameters of human skin in vivo. Biomech Model Mechanobiol 8(1):1–8
88. Meijer RR, Douven LL, Oomens CC (1999) Characterisation of anisotropic and non-linear behaviour of human skin in vivo. Comput Methods Biomech Biomed Eng 2(1):13–27
89. Groves RB, Coulman S, Birchall J, Evans SL (2013) An anisotropic, hyperelastic model for skin: experimental measurements, finite element modelling and identification of parameters for human and murine skin. J Mech Behav Biomed Mater 18:167–180
90. Rivlin R (1948) Large elastic deformations of isotropic materials. IV. Further developments of the general theory. Phil Trans R Soc A 241(835):379–397
91. Ogden R (1972) Large deformation isotropic elasticity – on the correlation of theory and experiment for incompressible rubberlike solids. Proc R Soc Lond A Math Phys Sci 326(1567):565–584
92. Tong P, Fung YC (1976) The stress-strain relationship for the skin. J Biomech 9(10):649–657

93. Weiss JA, Maker BN, Govindjee S (1996) Finite element implementation of incompressible, transversely isotropic hyperelasticity. Comput Methods Appl Mech Eng 135:107–128
94. Bischoff JE, Arruda EM, Grosh K (2000) Finite element modeling of human skin using an isotropic, nonlinear elastic constitutive model. J Biomech 33(6):645–652
95. Limbert G (2011) A mesostructurally-based anisotropic continuum model for biological soft tissues–decoupled invariant formulation. J Mech Behav Biomed Mater 4(8):1637–1657
96. Flynn C, Rubin MB, Nielsen PMF (2011) A model for the anisotropic response of fibrous soft tissues using six discrete fibre bundles. Int J Numer Meth Biomed Eng 27(11):1793–1811
97. Avril S (2017) Overview of identification methods of mechanical parameters based on full-field measurements. In: Avril S, Evans S (eds) Material parameter identification and inverse problems in soft tissue biomechanics, vol 573. Springer, Cham, pp 37–66
98. Koziel S, Yang X-S (2011) Computational optimization, methods and algorithms. Springer, Berlin Heidelberg
99. Conn AR, Scheinberg K, Vicente LN (2009) Introduction to derivative-free optimization. SIAM, Philadelphia
100. Lagarias JC, Reeds JA, Wright MH, Wright PE (1998) Convergence properties of the Nelder-Mead simplex method in low dimensions. SIAM J Optim 9(1):112–147
101. Nelder JA, Mead R (1965) A simplex method for function minimization. Comput J 7:308–313
102. Hendriks F, Brokken D, Oomens C, Baaijens F (2004) Influence of hydration and experimental length scale on the mechanical response of human skin in vivo, using optical coherence tomography. Skin Res Technol 10(4):231–241
103. Jor JWY, Nash MP, Nielsen PMF, Hunter PJ (2011) Estimating material parameters of a structurally based constitutive relation for skin mechanics. Biomech Model Mechanobiol 10(5):767–778
104. Avril S, Bonnet M, Bretelle A-S, Grédiac M, Hild F, Ienny P, Latourte F et al (2008) Overview of identification methods of mechanical parameters based on full-field measurements. Exp Mech 48:381–402